

NASA TM X-322

GR  
Doc  
Int  
Ext

GPO PRICE \$ \_\_\_\_\_

CFSTI PRICE(S) \$ \_\_\_\_\_

Hard copy (HC) \$2.00

Microfiche (MF) .50



FACILITY FORM 502

N66-20901

(ACCESSION NUMBER)

(PAGES)

TMX 302  
(NASA CR OR TMX OR AD NUMBER)

Copy

631

NASA TM X-322

(THRU)

(CODE)

(CATEGORY)

ff 653 July 65

# TECHNICAL MEMORANDUM

X-322

DECLASSIFIED- AUTHORITY  
US: 663 DROBKA TO LEBOW  
MEMO DATED 2/1/66  
1/10/66

AERODYNAMIC CHARACTERISTICS IN PITCH AT A MACH NUMBER  
OF 1.97 OF TWO VARIABLE-WING-SWEEP V/STOL  
CONFIGURATIONS WITH OUTBOARD WING PANELS  
SWEEPED BACK 75°

By Gerald V. Foster and Odell A. Morris

Langley Research Center  
Langley Field, Va.

Declassified by authority of NASA  
Classification Change Notices No. 50  
Dated \*\* 2/16/66

NATIONAL AERONAUTICS AND SPACE ADMINISTRATION  
WASHINGTON

October 1960

TECHNICAL MEMORANDUM X-322

AERODYNAMIC CHARACTERISTICS IN PITCH AT A MACH NUMBER  
OF 1.97 OF TWO VARIABLE-WING-SWEEP V/STOL  
CONFIGURATIONS WITH OUTBOARD WING PANELS  
SWEEP BACK 75°\*

By Gerald V. Foster and Odell A. Morris

SUMMARY

20901

L  
1  
1  
7  
8

An investigation has been conducted in the Langley 4- by 4-foot supersonic pressure tunnel at a Mach number of 1.97 to determine the aerodynamic characteristics in pitch of two variable-wing-sweep V/STOL configurations with the outboard wing panels swept back 75°.

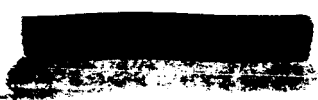
The results show a linear variation of pitching moment with lift coefficient for both models tested. These results, in conjunction with results for the same models at subsonic and transonic speeds obtained from NASA Technical Memorandum X-321, indicate that the total change in static margin due to increasing the Mach number and changing the wing sweep from 25° to 75° is about 13 percent of the mean geometric chord. The maximum untrimmed lift-drag ratios for the complete configurations were 4.20 for model 1 and 3.75 for model 2.

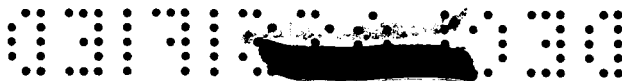
*Quest 9*

INTRODUCTION

Several current investigations have indicated that airplane configurations employing variable-wing sweep appear to provide a satisfactory means of combining efficient subsonic and supersonic flight characteristics into one airplane. (See refs. 1 to 4.) Recent studies have also indicated the feasibility of employing rotatable jet-exit nozzles to provide short- or vertical-take-off-and-landing capabilities. As a result of these studies, it appears desirable to combine both design concepts into one configuration to provide more efficient flight characteristics for an STOL- or VTOL-type aircraft. Thus, an investigation is currently

\*Title, Unclassified.





being conducted by the National Aeronautics and Space Administration to determine the aerodynamic characteristics of several model configurations designed to simulate an STOL-type aircraft with variable-sweep wings. These configurations would also have vertical-take-off capabilities for light load conditions and were designed for speeds up to a Mach number of 2.5.

The results presented herein include the aerodynamic characteristics in pitch for two model configurations that were tested in the Langley 4-by 4-foot supersonic pressure tunnel. One model would provide short-field- or vertical-take-off capabilities with the use of four nozzles angled downward; whereas the second model configuration employs only three nozzles. The same variable-sweep-wing design with a leading-edge sweep of  $75^\circ$  on the outer panels was used on both models and is identical to one of the wings reported in reference 3. Tests were made of the complete configurations and of the various combinations of components at a Mach number of 1.97 with a corresponding Reynolds number, based on the wing mean geometric chord, of  $1.31 \times 10^6$ .

#### SYMBOLS

The forces and moments are referred to the wind-axis system. The moment reference of models 1 and 2 is located on the body center line at 52.1-percent and 51.4-percent body length, respectively. The coefficients and symbols are defined as follows:

$C_D$  drag coefficient,  $\frac{\text{Drag}}{qS}$

$C_{D,i}$  internal-drag coefficient of ducts,  $\frac{\text{Internal drag}}{qS}$

$C_L$  lift coefficient,  $\frac{\text{Lift}}{qS}$

$C_m$  pitching-moment coefficient,  $\frac{\text{Pitching moment}}{qS\bar{c}}$

$\bar{c}$  wing mean geometric chord, 1.302 ft

$L/D$  lift-drag ratio,  $\frac{C_L}{C_D}$



M free-stream Mach number

q free-stream dynamic pressure, lb/sq ft

S wing area including fuselage intercept, 2.449 sq ft

$\alpha$  angle of attack, deg

$\delta_h$  horizontal-tail control deflection, deg

$\Lambda_{LE}$  leading-edge sweepback angle, deg

Components:

W wing

B body

V vertical fin

H horizontal tail

# MODELS AND APPARATUS

The models used in these tests (referred to herein as models 1 and 2) differed only in body and tail design. Details of the models are shown in figure 1 and photographs are presented in figure 2. The body of model 1 had two scoop-type inlets (capture area of 6.72 sq in.) located on the sides of the forebody. These inlets were connected to two pairs of jet exits located beneath the wing on both sides of the body. The angle formed in the horizontal plane by the axis of the jet exit and the body center line was  $27\frac{1}{2}^\circ$  and the area of each exit was 3.30 sq in. The horizontal and vertical tails of model 1 were constructed of 1/8-inch-thick sheet metal and had rounded leading edges (swept back  $45^\circ$ ) and beveled trailing edges. The horizontal tail of model 1 had a taper ratio of 0.30 and an aspect ratio of 1.5. The vertical tail had a taper ratio of 0.30 and an aspect ratio of 1.28.

The body of model 2 differed from the body of model 1 only in the section behind the forward set of inlets. The rear jet exits of model 1 were replaced with a single exit, with an area of 6.72 sq in., at the base of the body. It may be noted from figures 2(a) and 2(c) that the cutout for the base exit of model 2 was appreciably larger than the cutout required for the support sting of model 1. The area of the jet exit

037155:030

located on the side of the body of model 2 was 3.50 sq in. Both the horizontal and vertical tail of model 2 had 60° sweptback leading edges and a taper ratio of 0.18. The aspect ratio was 1.26 for the horizontal tail and 0.86 for the vertical tail.

The same wing was used with both bodies. The leading-edge sweepback angle of the inboard wing section was 60°; whereas the sweepback angle of outboard sections was 75°. With the outboard wing panels swept back 25°, the outboard airfoil sections were NACA 65A006, and the airfoil sections for the inboard wing panel were NACA 65A004.5 in a plane parallel to the free stream. The wing was mounted 2.90 inches above the body center line with zero incidence and dihedral.

#### TESTS, CORRECTIONS, AND ACCURACY

The test conditions are as follows:

Mach number . . . . .	1.97
Stagnation temperature, °F . . . . .	100
Stagnation pressure, lb/sq in. . . . .	4
Reynolds number based on $\bar{c}$ . . . . .	$1.31 \times 10^6$

The stagnation dewpoint was maintained sufficiently low (-25° or less) so that no condensation effects were encountered in the test section. Tests were made for an angle-of-attack range of -4° to 12°. The angles of attack were corrected for the deflection of the balance and sting under load. The base pressure was measured and the drag force was adjusted to a base pressure equal to free-stream static pressure. The drag and lift data were corrected to remove the contribution of internal drag due to the body internal flow. In order to insure a turbulent boundary layer, 1/8-inch-wide strips of No. 60 carborundum grains were attached to the wing and tail surfaces at the 0.10-chord station and around the fuselage 3.5 inches rearward of the nose.

The estimated accuracy of the measured quantities is as follows:

$C_D$ . . . . .	$\pm 0.0010$
$C_L$ . . . . .	$\pm 0.0050$
$C_m$ . . . . .	$\pm 0.0015$
$\alpha$ , deg . . . . .	$\pm 0.1$
$\delta_h$ , deg . . . . .	$\pm 0.1$

L  
1  
1  
7  
8

DECLASSIFIED

5

## PRESENTATION OF RESULTS

The results of the investigation and the figures in which they will be found are shown in the following table:

	Figure
Variation of internal-drag coefficient with angle of attack for models 1 and 2 . . . . .	3
Aerodynamic characteristics in pitch for various combinations of components for model 1 . . . . .	4
Effect of horizontal-tail deflection on the aerodynamic characteristics in pitch for the complete configuration of model 1 . . .	5
Aerodynamic characteristics in pitch for various combinations of components for model 2 . . . . .	6
Effect of horizontal-tail deflection on the aerodynamic characteristics in pitch for the complete configuration of model 2 . . . . .	7

## SUMMARY OF RESULTS

A comparison of the results presented in figures 5 and 7 indicates that the pitching moments of both models varied linearly with  $C_L$ , and the slope  $\partial C_m / \partial C_L$  was -0.19 for model 1 and -0.17 for model 2. These results, in conjunction with results for the same models at subsonic and transonic speeds (ref. 5), indicate that the total change in static margin due to increasing the Mach number from 0.60 to 1.97 and changing the wing sweep from  $25^\circ$  to  $75^\circ$  is about 13 percent of the mean geometric chord. The pitching-moment coefficient at zero lift of the wing-body configurations indicates a value of about -0.02 for model 1 (fig. 4(a)) and about zero for model 2 (fig. 6(a)). This negative pitching-moment increment for model 1 is associated with a rearward shift of wing center of pressure resulting from the effects of the four jet exits on the wing lower-surface pressures. The addition of the horizontal tail to model 1 provided a substantial positive increment in pitching moment at  $C_L = 0$ ; whereas adding the horizontal tail to model 2 resulted in no appreciable change in pitching moment at zero lift. It should be pointed out, however, that the pitching-moment characteristics for both models may be affected by the proximity of the support sting.

A comparison of the drag characteristics of model 1 (fig. 4(b)) with those of model 2 (fig. 6(b)) indicates that the minimum drag of model 1 (0.0400) was 0.0010 less than that of model 2. It should be pointed out,

CONFIDENTIAL

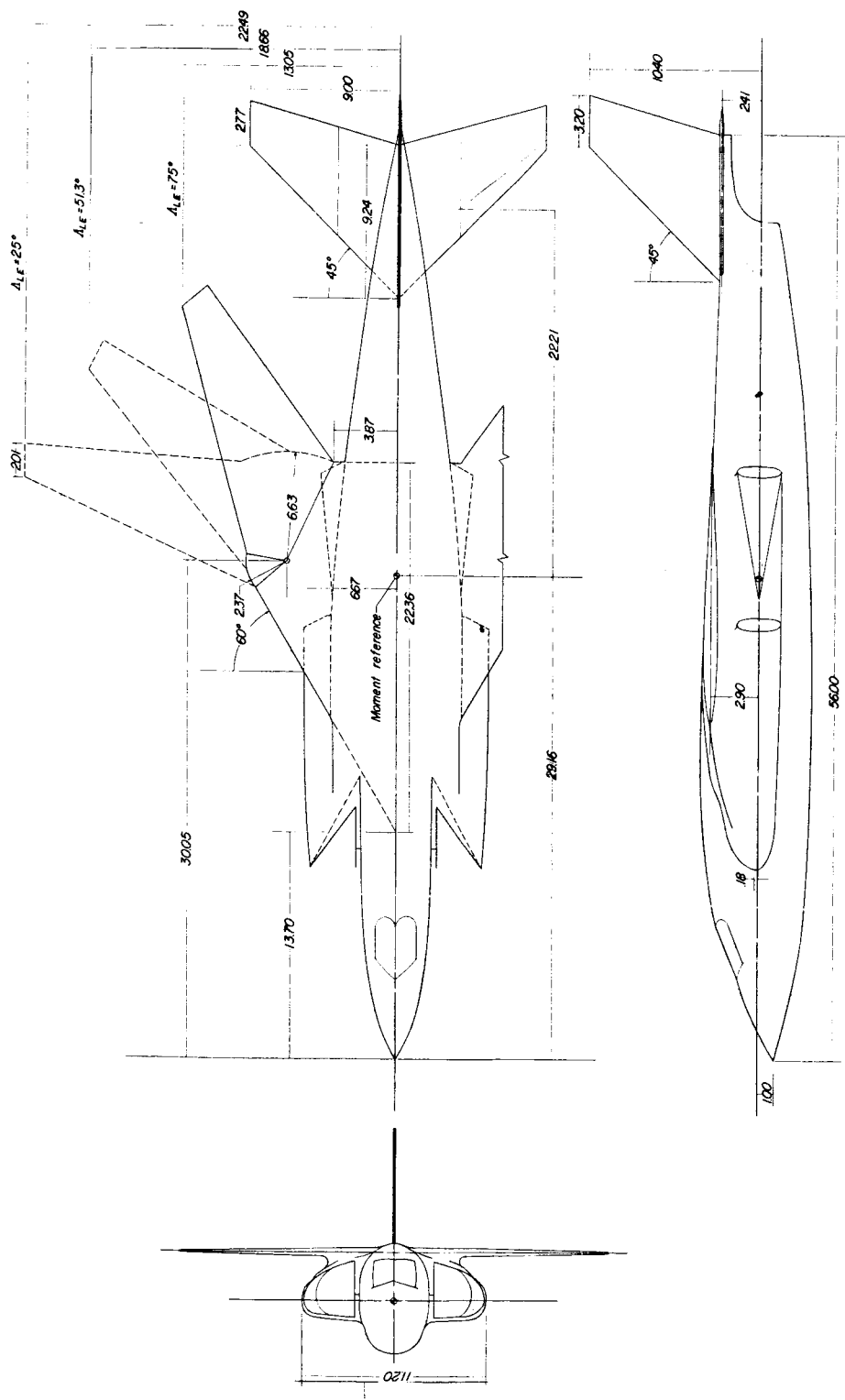
however, that the internal-drag coefficient was approximately 0.0160 for model 1 and 0.0120 for model 2. The maximum untrimmed lift-drag ratio of model 1 (4.20) is slightly higher than that for model 2 (3.75), and the relatively low maximum L/D of both models is due to the large values of minimum drag.

Langley Research Center,  
National Aeronautics and Space Administration,  
Langley Field, Va., June 6, 1960.

#### REFERENCES

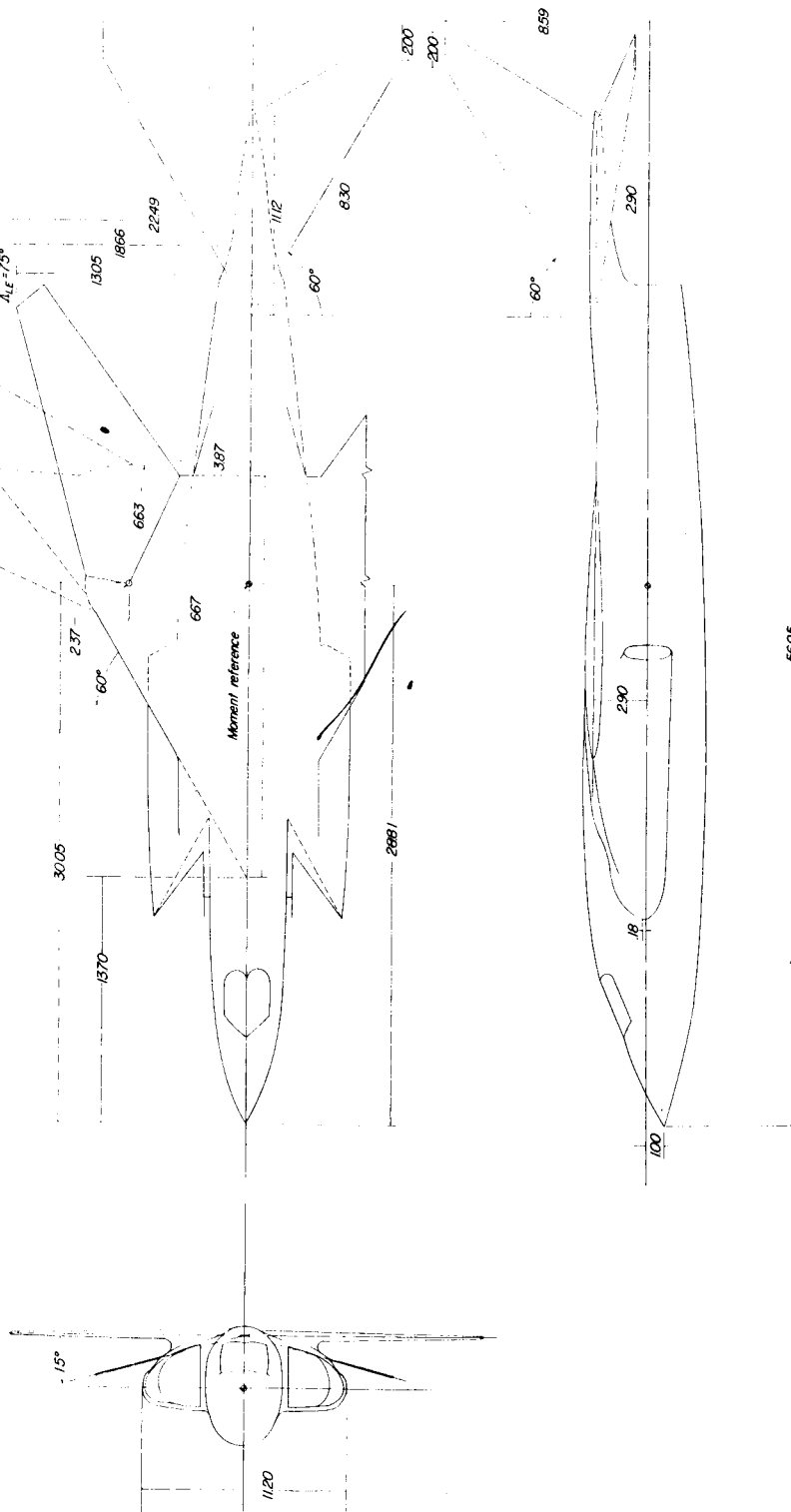
1. Alford, William J., Jr., and Henderson, William P.: An Exploratory Investigation of the Low-Speed Aerodynamic Characteristics of Variable-Wing-Sweep Airplane Configurations. NASA TM X-142, 1959.
2. Spearman, M. Leroy, and Foster, Gerald V.: Stability and Control Characteristics at a Mach Number of 2.01 of a Variable-Wing-Sweep Configuration With Outboard Wing Panels Swept Back  $75^{\circ}$ . NASA TM X-32, 1959.
3. Spencer, Bernard, Jr.: Stability and Control Characteristics at Low Subsonic Speeds of an Airplane Configuration Having Two Types of Variable-Sweep Wings. NASA TM X-303, 1960.
4. Bielat, Ralph P., Robins, A. Warner, and Alford, William J., Jr.: The Transonic Aerodynamic Characteristics of Two Variable-Sweep Airplane Configurations Capable of Low-Level Supersonic Attack. NASA TM X-304, 1960.
5. Luoma, Arvo A., and Alford, William J., Jr.: Performance, Stability, and Control Characteristics at Transonic Speeds of Three Z/STOL Airplane Configurations With Wings of Variable Sweep. NASA TM X-321, 1960.

L  
1  
1  
7  
8



(a) Model 1.

Figure 1.- Details of model. All dimensions in inches unless otherwise noted.



(b) Model 2.

Figure 1.- Concluded.

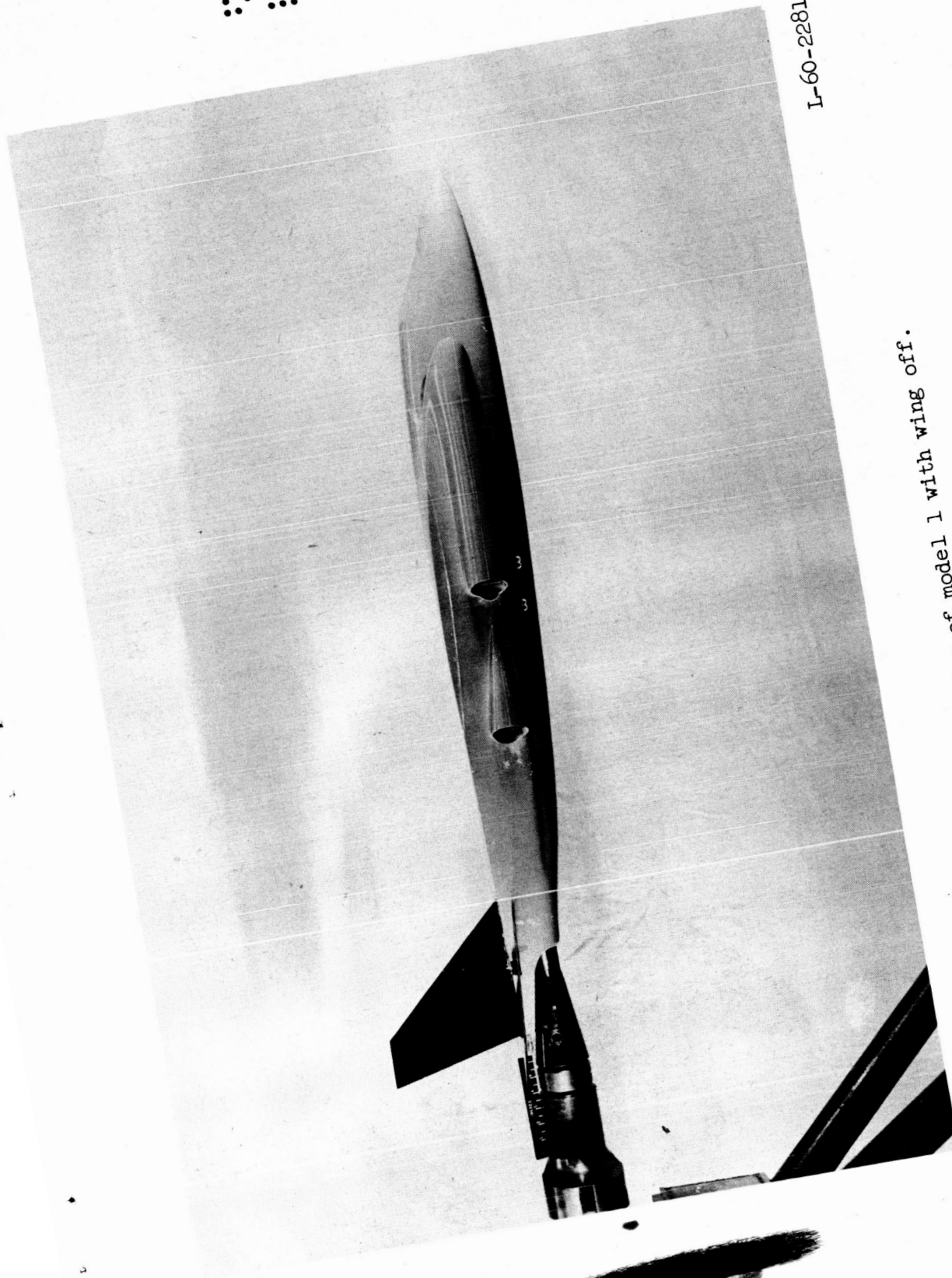
2G

1-1110

DECLASSIFIED

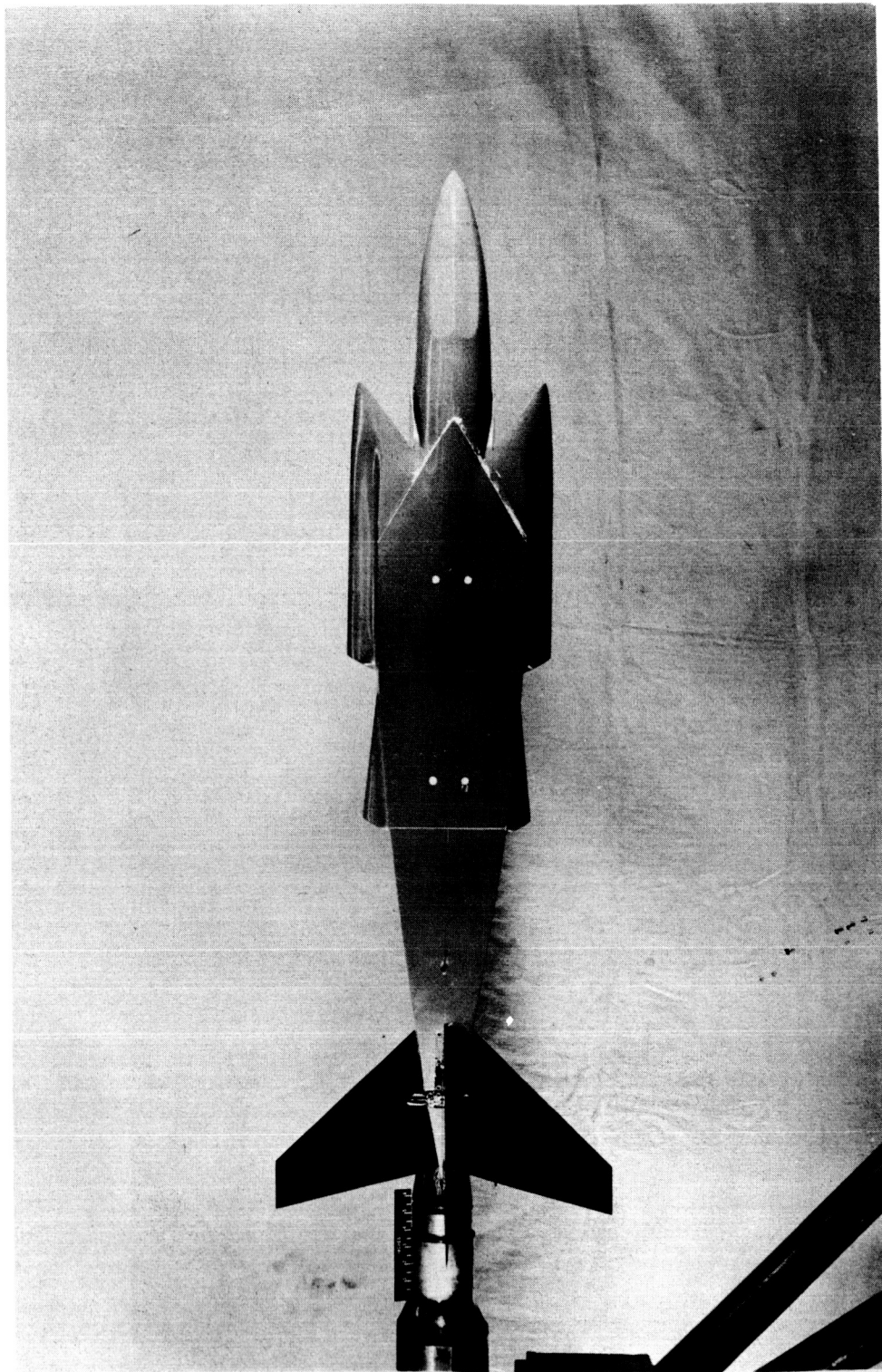
9

L-60-2281



(a) Side view of model 1 with wing off.

Figure 2.- Photographs of models.

0373 ~~SECRET~~ 33

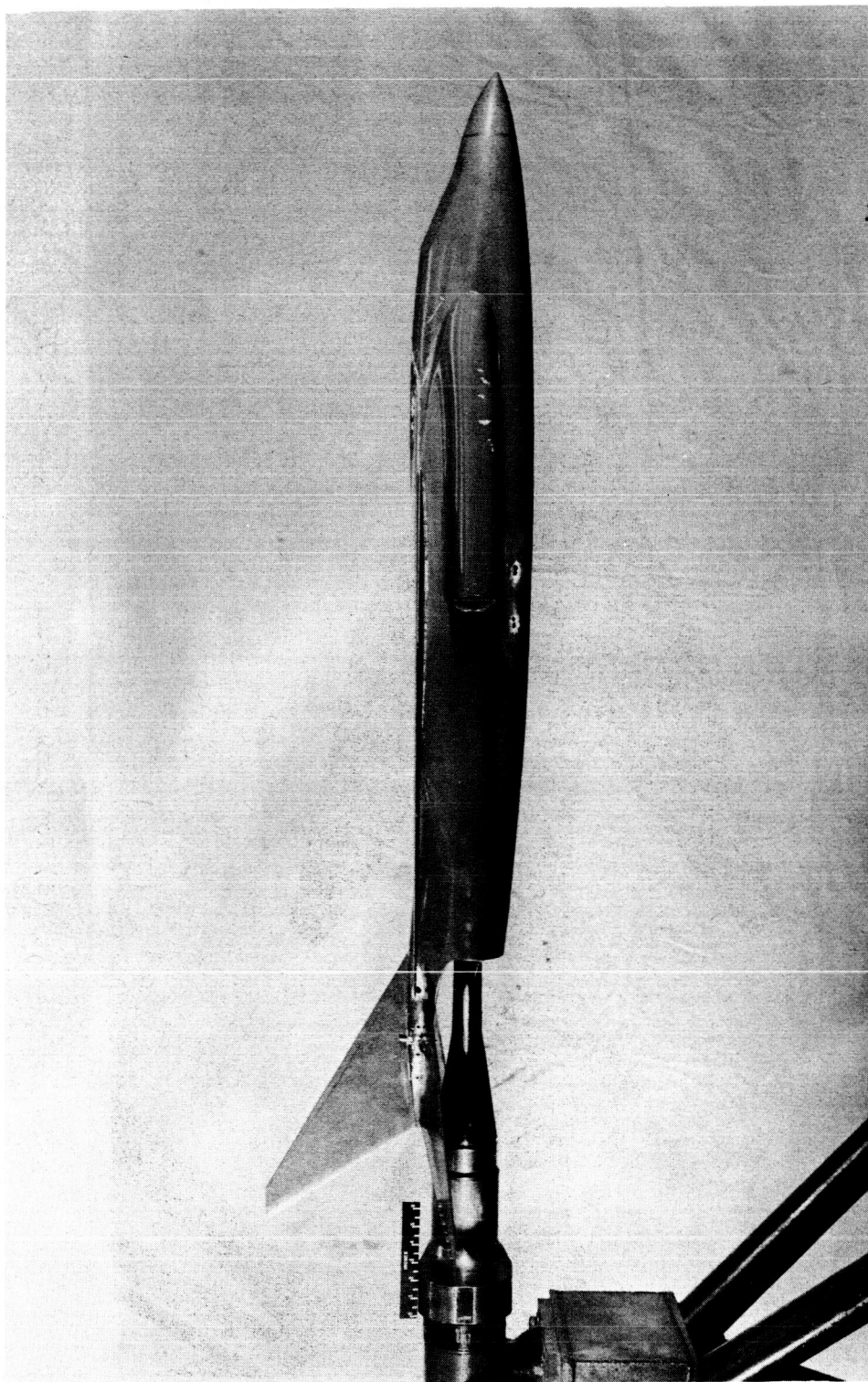
L-60-2280

(b) Top view of model 1 with wing off.

Figure 2.- Continued.

DECLASSIFIED

11



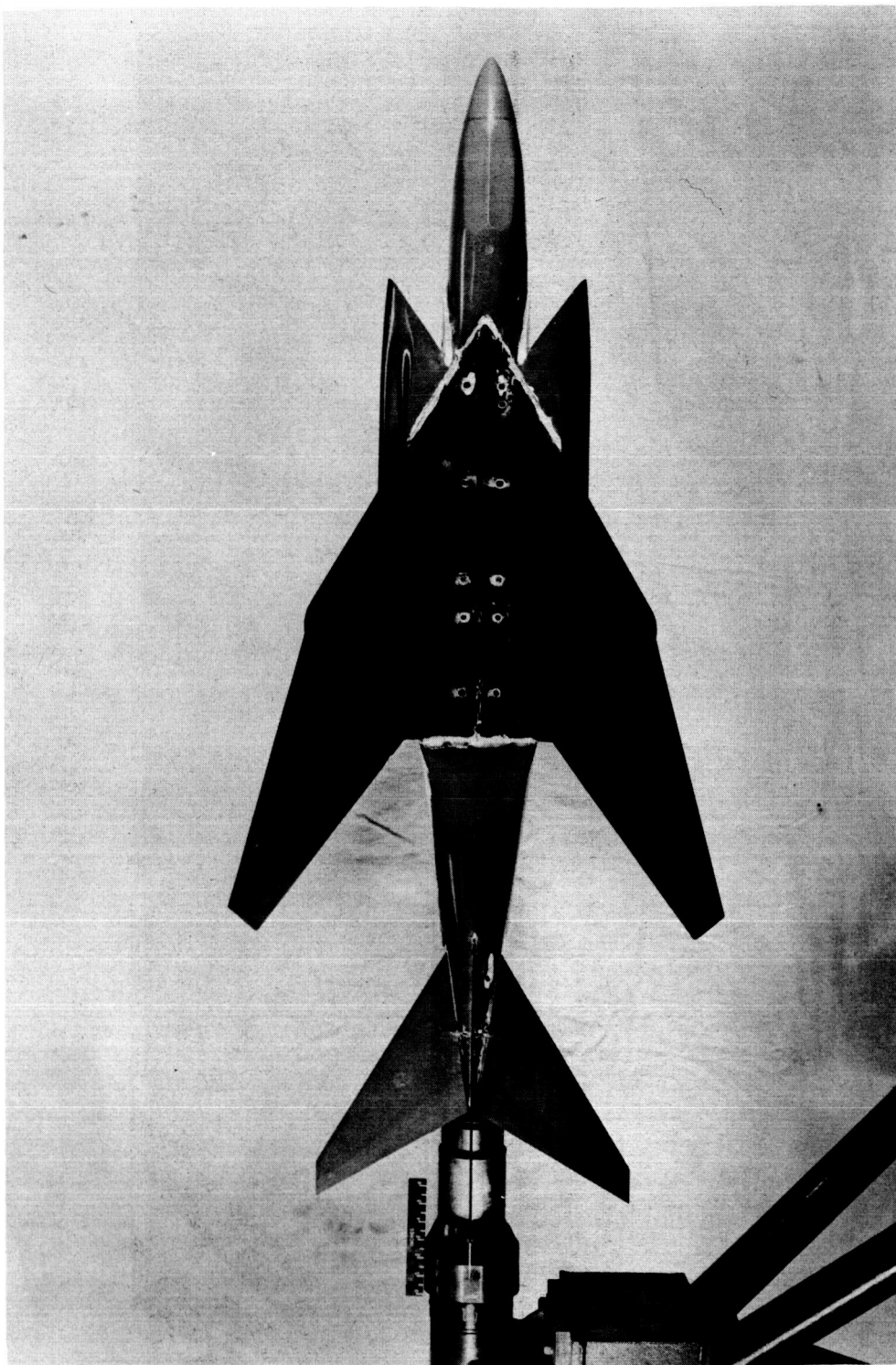
L-60-2284

(c) Side view of model 2.

Figure 2.- Continued.

L-1178

037134 030

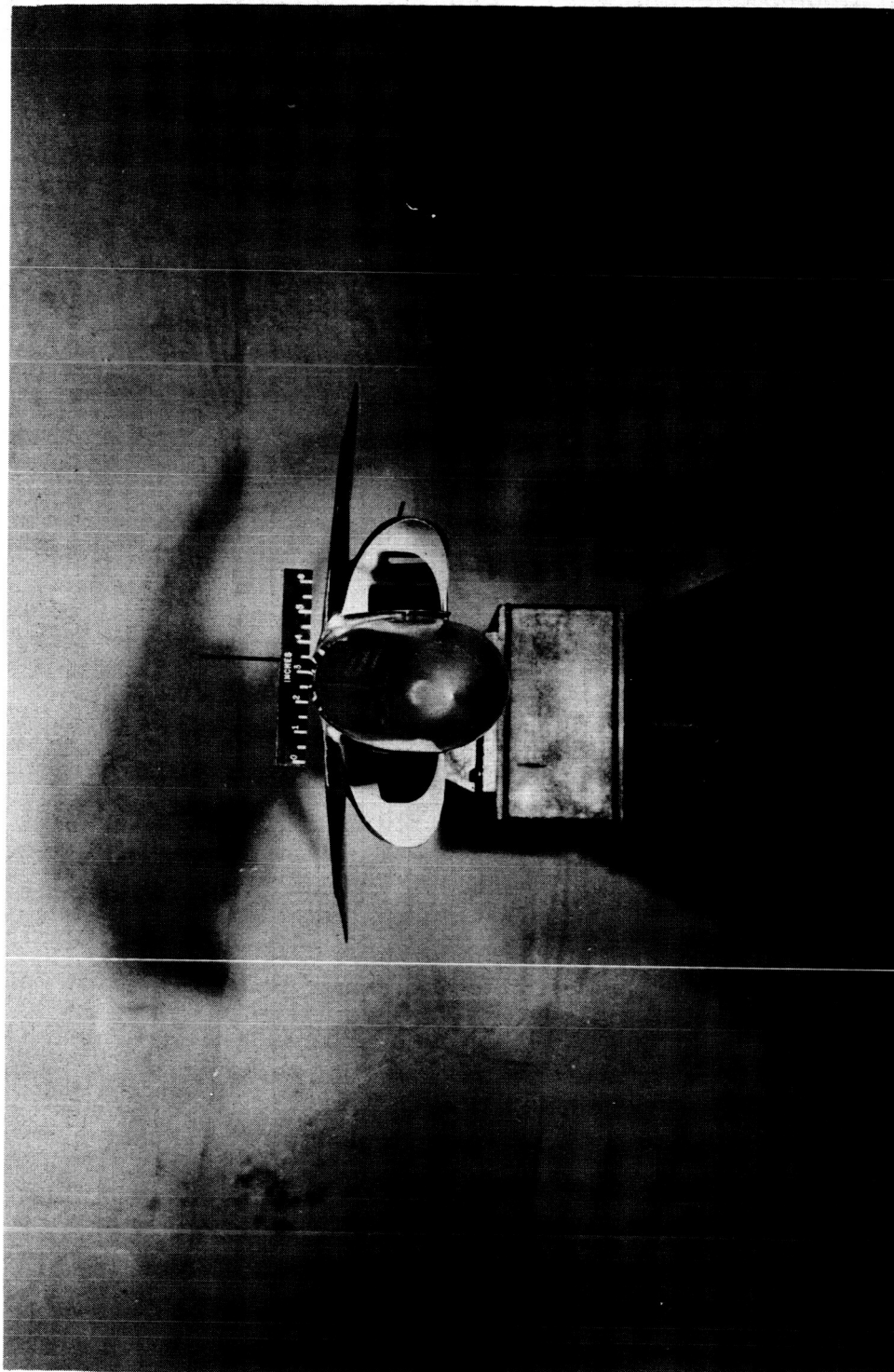


(d) Top view of model 2. L-60-2279

Figure 2.- Continued.

DECLASSIFIED

13



(e) Front view of model 2. L-60-2283

Figure 2.- Concluded.

L-1178

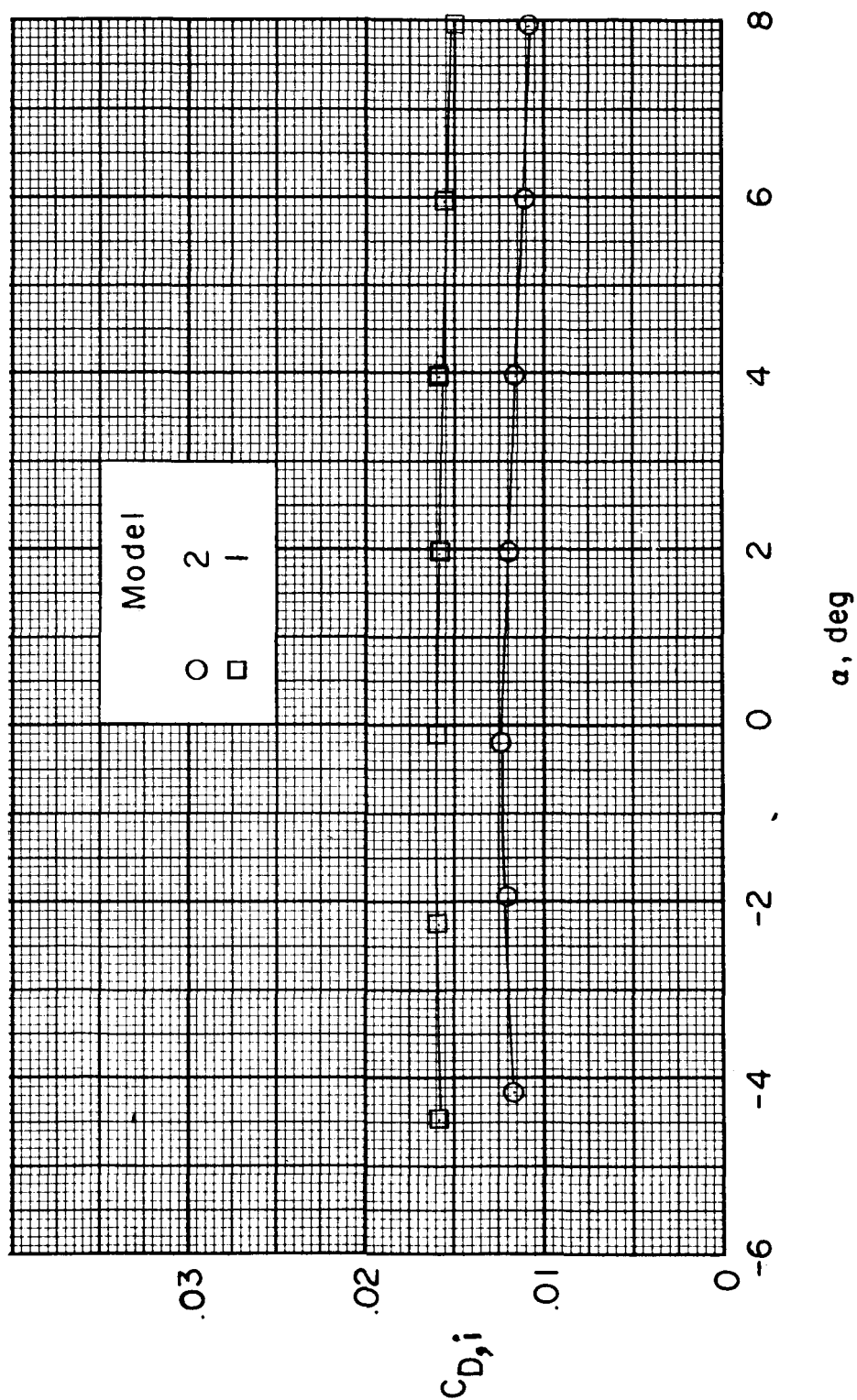
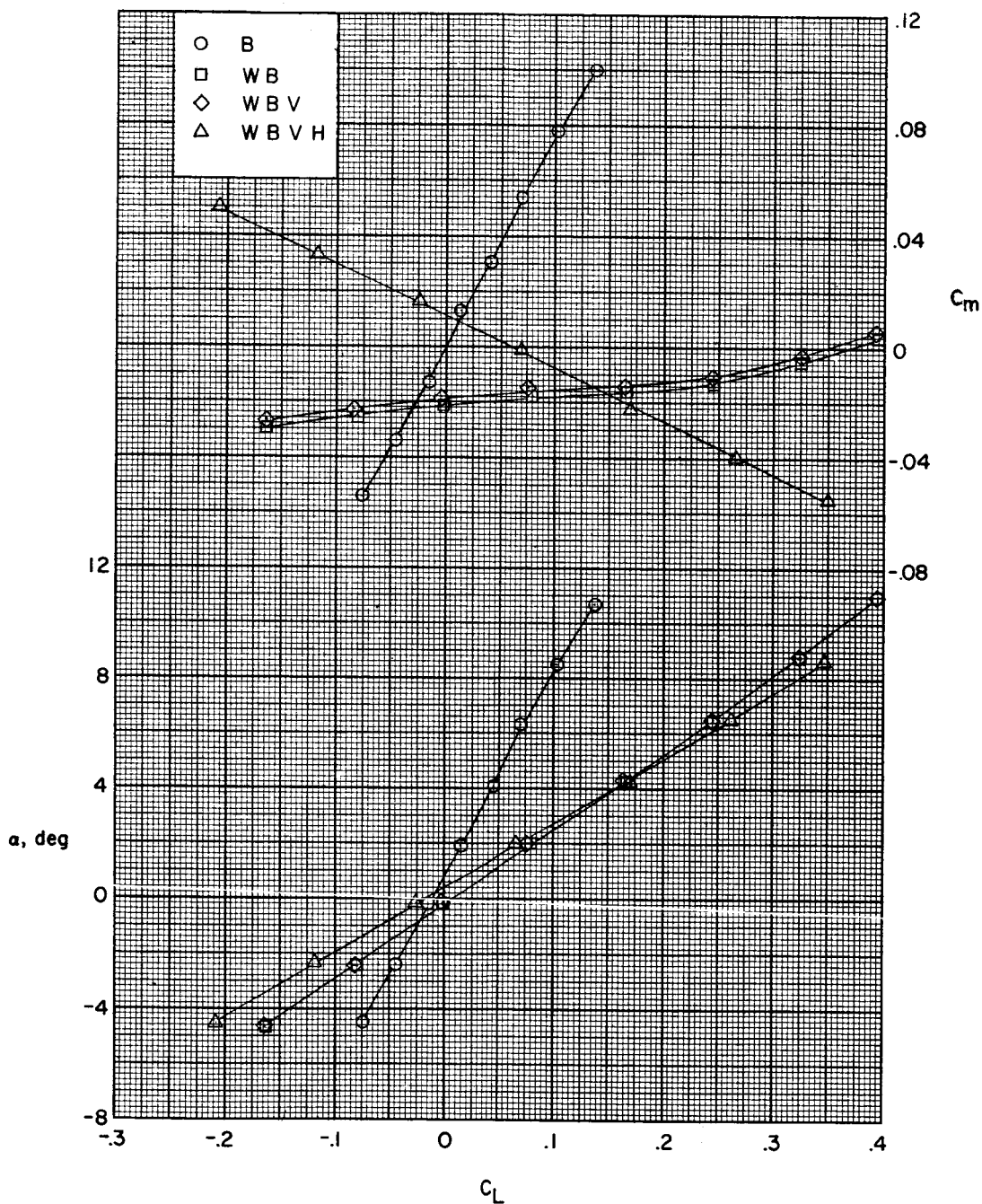


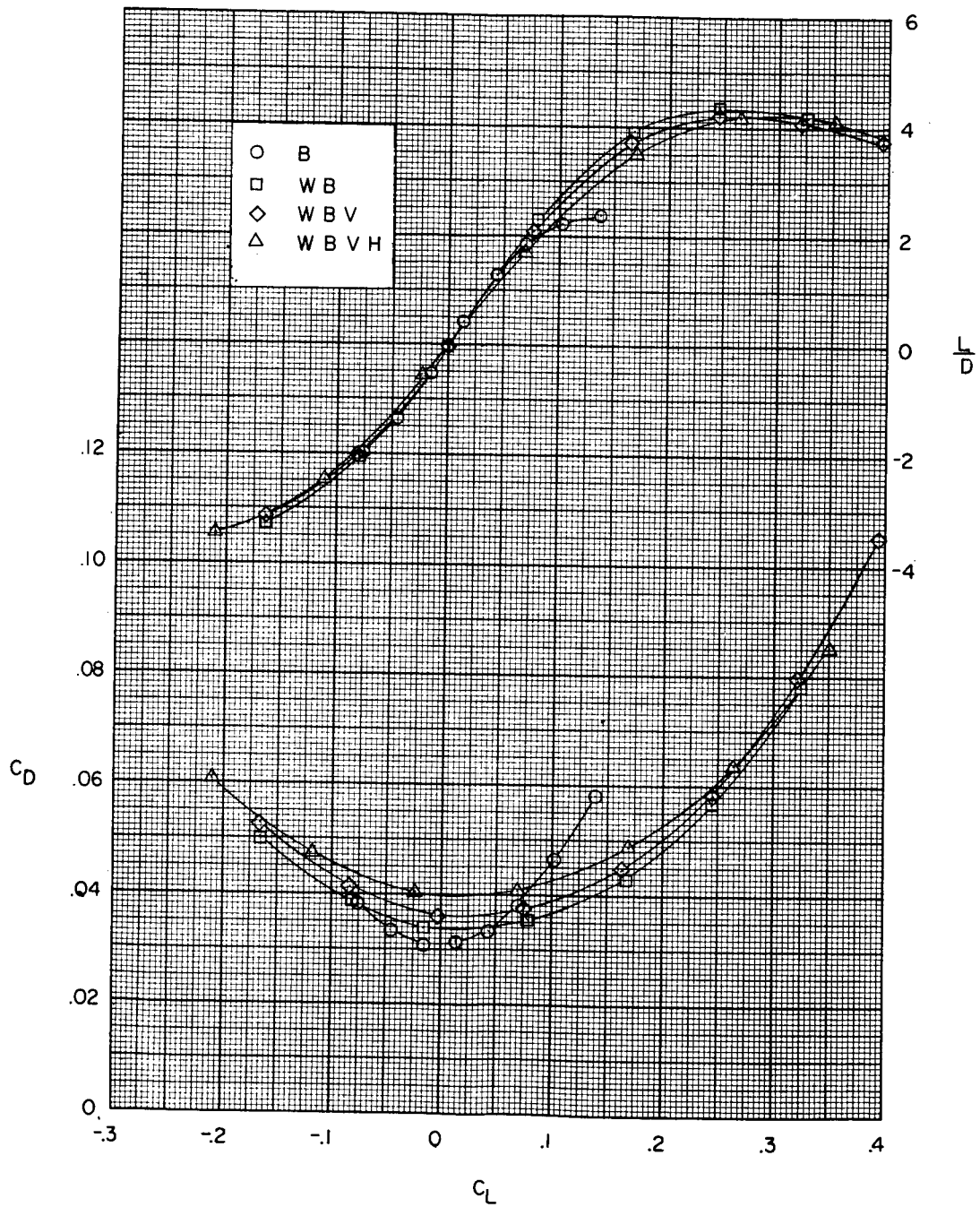
Figure 3.- Variation of internal-drag coefficient with angle of attack for models 1 and 2.



(a) Variation of  $C_m$  and  $\alpha$  with  $C_L$ .

Figure 4.- Aerodynamic characteristics in pitch for various combinations of components for model 1.

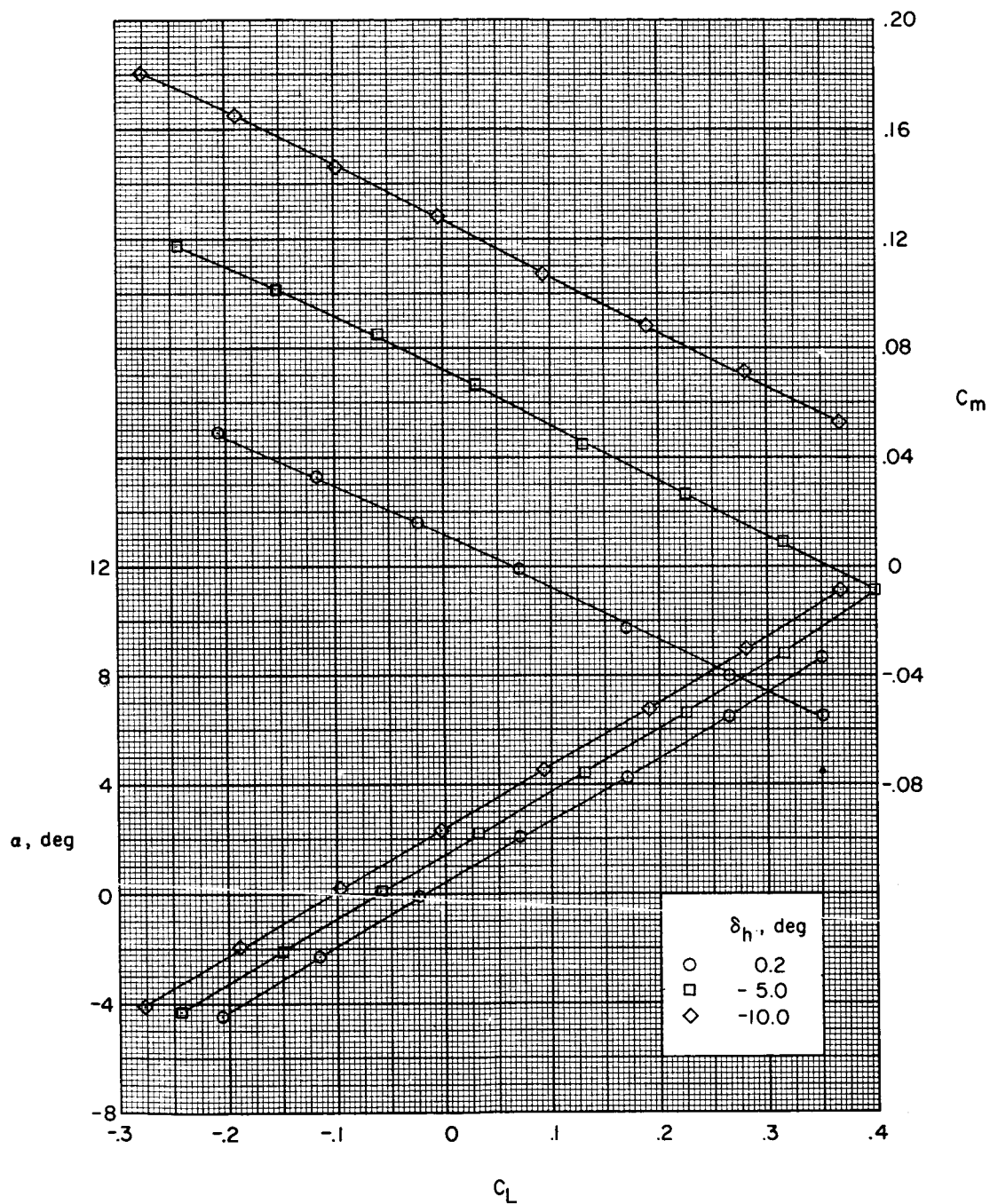
037: [REDACTED] 030



(b) Variation of  $L/D$  and  $C_D$  with  $C_L$ .

Figure 4.- Concluded.

L-1178

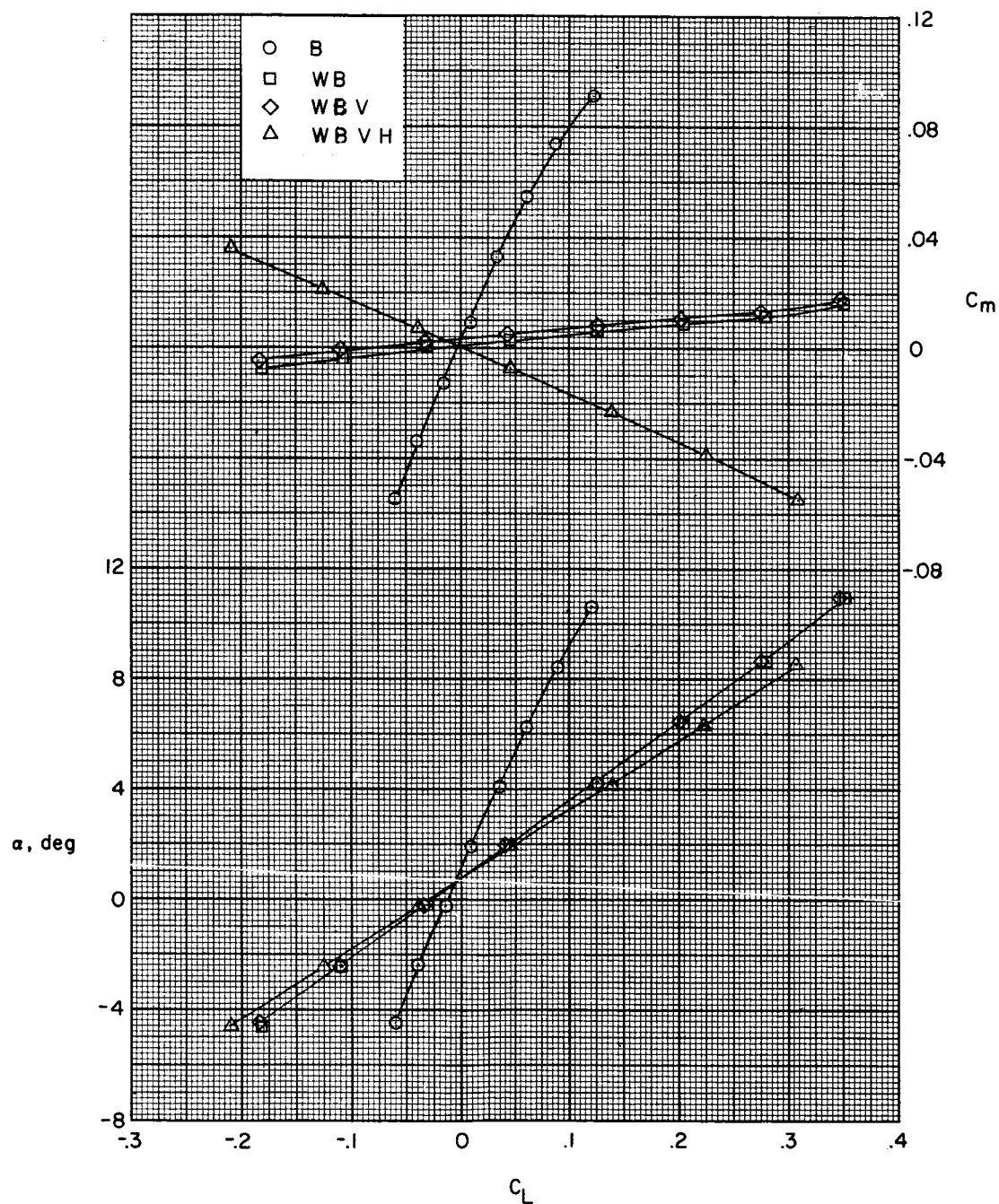


(a) Variation of  $C_m$  and  $\alpha$  with  $C_L$ .

Figure 5.- Effect of horizontal-tail deflection on the aerodynamic characteristics in pitch for the complete configuration of model 1.



SECRET

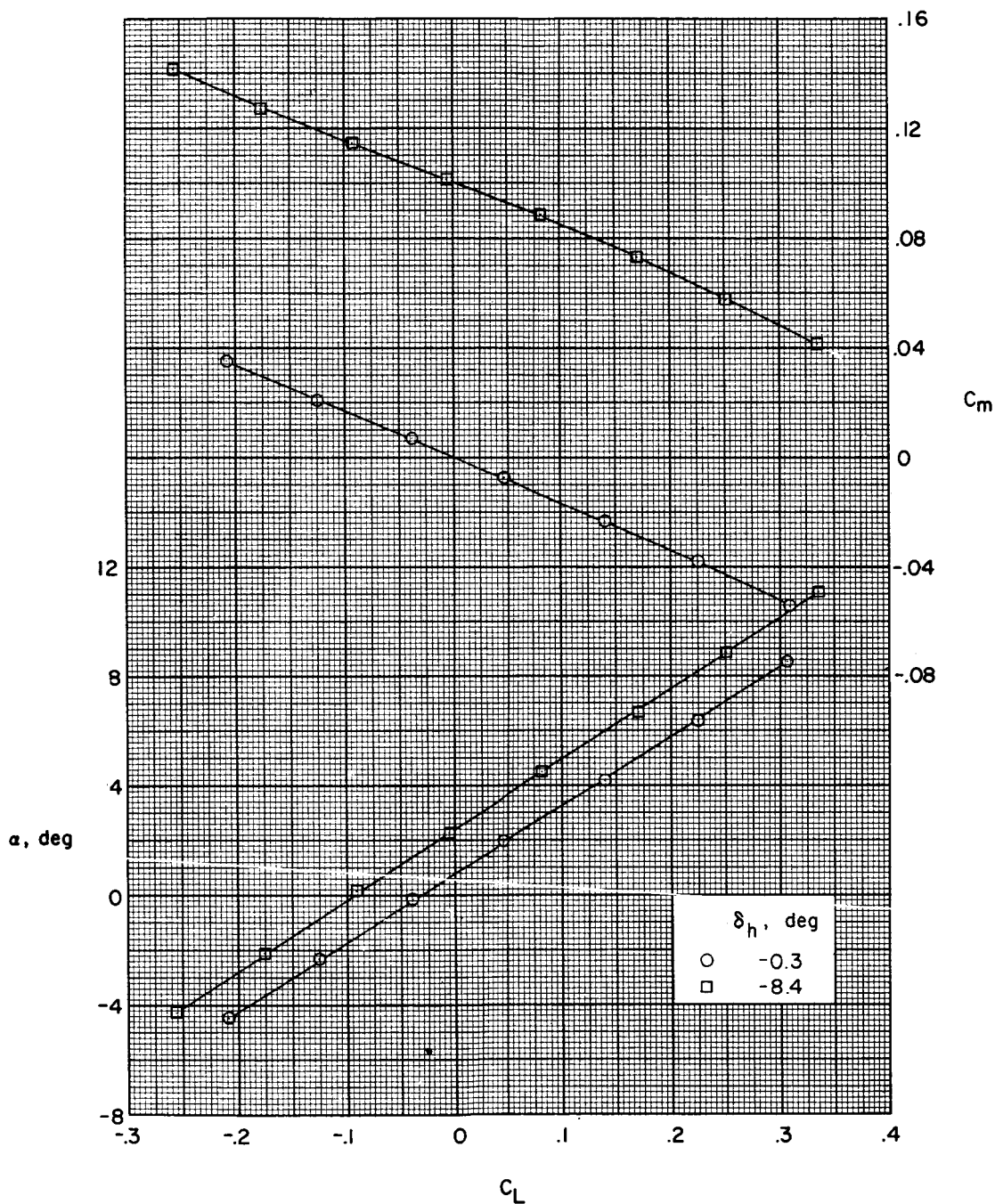


(a) Variation of  $C_m$  and  $\alpha$  with  $C_L$ .

Figure 6.- Aerodynamic characteristics in pitch for various combinations of components for model 2.

SECRET

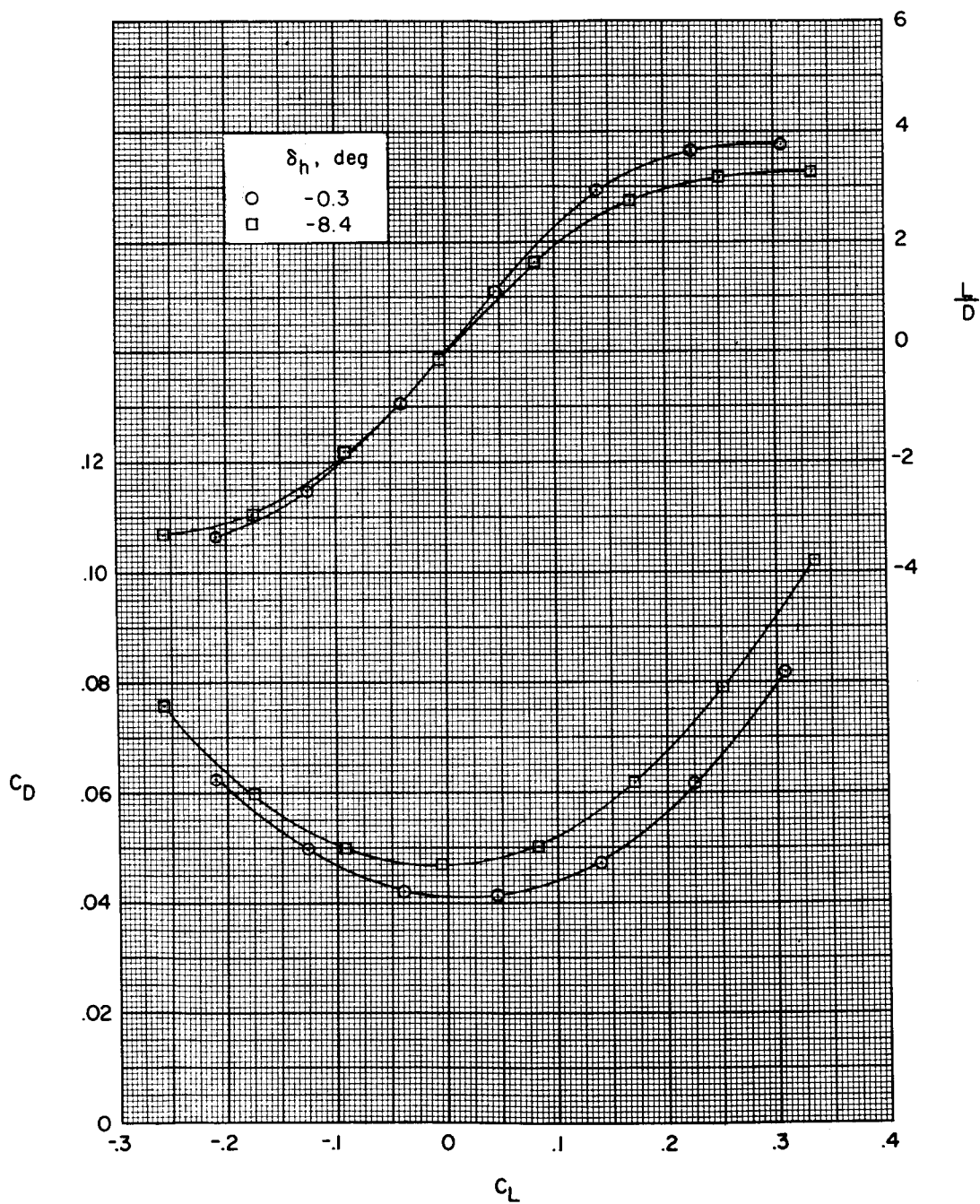




(a) Variation of  $C_m$  and  $\alpha$  with  $C_L$ .

Figure 7.- Effect of horizontal-tail deflection on the aerodynamic characteristics in pitch for the complete configuration of model 2.

0378 [REDACTED] 039



(b) Variation of  $L/D$  and  $C_D$  with  $C_L$ .

Figure 7.- Concluded.